



European Research Infrastructure supporting Smart Grid Systems Technology Development, Validation and Roll Out

Technical Report TA User Project **Smart beats Copper**

Grant Agreement No:	654113
Funding Instrument:	Research and Innovation Actions (RIA) – Integrating Activity (IA)
Funded under:	INFRAIA-1-2014/2015: Integrating and opening existing national and regional research infrastructures of European interest
Starting date of project:	01.11.2015
Project Duration:	54 month

Contractual delivery date:	31/10/2018
Actual delivery date:	31/10/2018
Name of lead beneficiary for this deliverable:	Prof. Gerd Heilscher, Ulm University of Applied Sciences
Deliverable Type:	Report (R)
Security Class:	Public (PU)
Revision / Status:	released

Document Information

Document Version: 3
Revision / Status: released

All Authors/Partners Basem Idlbi, Falko Ebe, Christoph Kondzialka, Matthias Casel, Shuo Chen, Gerd Heilscher

Distribution List ERIGrid Consortium Members

Document History

Revision	Content / Changes	Resp. Partner	Date
1	Initial Structure and Content	HSU	12.09.18
2	Content System Setups and Results	HSU	19.09.18
3	Content	HSU	22.10.18

Document Approval

Final Approval	Name	Resp. Partner	Date
Review Steering Com. Level	Thomas Strasser	AIT	31.10.18

Disclaimer

This document contains material, which is copyrighted by certain ERIGrid consortium parties and may not be reproduced or copied without permission. The information contained in this document is the proprietary confidential information of certain ERIGrid consortium parties and may not be disclosed except in accordance with the consortium agreement.

The commercial use of any information in this document may require a licence from the proprietor of that information.

Neither the ERIGrid consortium as a whole, nor any single party within the ERIGrid consortium warrant that the information contained in this document is capable of use, nor that the use of such information is free from risk. Neither the ERIGrid consortium as a whole, nor any single party within the ERIGrid consortium accepts any liability for loss or damage suffered by any person using the information.

This document does not represent the opinion of the European Community, and the European Community is not responsible for any use that might be made of its content.

Copyright Notice

© The ERIGrid Consortium, 2015 – 2020

Table of contents

Executive Summary	6
1 General Information of the User Project	7
2 Research Motivation	8
2.1 Objectives	8
2.2 Scope	8
3 State-of-the-Art	9
4 Executed Tests and Experiments.....	10
4.1 Test Plan	10
4.2 Case Study	11
4.3 Test Set-up(s)	13
4.4 Data Management and Processing	15
5 Results and Conclusions.....	17
5.1 Comparison of the transient behaviour of the system setups	17
5.2 Comparison of the system behaviour to a voltage step	18
5.3 Comparison of the system behaviour to a voltage ramp.....	19
5.4 Case Study: Overlayed Voltage Control Algorithm.....	20
5.5 Evaluation of the cycle time of System Setup B.....	22
5.6 Conclusions	22
6 Open Issues and Suggestions for Improvements	25
7 Dissemination Planning	26
8 Annex	27
8.1 List of Figures	27
8.2 List of Tables	27
9 References	28
10 References to Technical Data Sheets	28

Abbreviations

<i>DER</i>	<i>Distributed Energy Resource</i>
<i>TA</i>	<i>Trans-national Access</i>
<i>CC</i>	<i>Correlation Coefficient</i>
<i>CFE</i>	<i>Communication Front End</i>
<i>CHIL</i>	<i>Controller Hardware-in-the-Loop</i>
<i>CLS</i>	<i>Controllable Local System</i>
<i>DA</i>	<i>Data Attribute (IEC 61850-specific)</i>
<i>DER</i>	<i>Distributed Energy Resources</i>
<i>DUT</i>	<i>Device-under-Test</i>
<i>DO</i>	<i>Data Object (IEC 61850-specific)</i>
<i>DRTS</i>	<i>Digital Real-Time Simulator</i>
<i>DS</i>	<i>Data Set (IEC 61850-specific)</i>
<i>DSO</i>	<i>Distribution System Operator</i>
<i>EDCC</i>	<i>Experimental Distribution Control Center</i>
<i>EMT</i>	<i>Electromagnetic Transient (Simulation)</i>
<i>EUT</i>	<i>Equipment-under-Test</i>
<i>HIL</i>	<i>Hardware-in-the-Loop</i>
<i>HUT</i>	<i>Hardware-under-Test</i>
<i>ICT</i>	<i>Information and Communication Technology</i>
<i>ICTHIL</i>	<i>Information-and-Communication-Technology-in-the-Loop</i>
<i>IED</i>	<i>Intelligent Electronic Device</i>
<i>IMD</i>	<i>Independent Measurement Device</i>
<i>IPCC</i>	<i>Intergovernmental Panel on Climate Change</i>
<i>LD</i>	<i>Logical Devices</i>
<i>LN</i>	<i>Logical Node (IEC 61850-specific)</i>
<i>ME</i>	<i>Mean Error</i>
<i>MEA</i>	<i>Measurement</i>
<i>MPPT</i>	<i>Maximum Power Point Tracking</i>
<i>OLTC</i>	<i>On-Load-Tap-Changer</i>
<i>PCC</i>	<i>Point of Common Coupling</i>
<i>PHIL</i>	<i>Power Hardware-in-the-Loop</i>
<i>PI</i>	<i>Power Interface</i>
<i>PV</i>	<i>Photovoltaic</i>
<i>RCB</i>	<i>Report Control Block (IEC 61850-specific)</i>
<i>RMS</i>	<i>Root Mean Square</i>
<i>RTU</i>	<i>Remote Terminal Unit</i>
<i>SCADA</i>	<i>Supervisory Control and Data Acquisition</i>
<i>SGAM</i>	<i>Smart Grid Architecture Model</i>

<i>SIL</i>	<i>Software-in-the-Loop</i>
<i>SMGW</i>	<i>Smart Meter Gateway</i>
<i>STD</i>	<i>Standard Deviation</i>
<i>SUT</i>	<i>System-under-Test</i>
<i>VPN</i>	<i>Virtual Private Network</i>

Executive Summary

The distributed generation of renewable energies imposes several challenges regarding grid resilience, such as voltage compliance or normal loading of some grid components. The energy transition towards renewable energies becomes a main driver for the design of grid control strategies and asset planning, which involves mostly the distribution level of grids, since it accommodates the highest rate of distributed generation. To mitigate potential problems in the grid, smart operation technologies must be undertaken, such as local self-control of distributed generators or centralized operation strategies, which are based on information and communication technologies (ICT). The Smart Grids Research Group at Ulm University of Applied Sciences (HSU) investigates several grid components and control strategies, especially PV inverters, their control strategies and communication interfaces, considering real grid data obtained from the grid operator in the area of Ulm. Such control strategies can be complex and requires many tests in laboratories, before they can be implemented at the level of end users. Nevertheless, simulating real grid conditions in a laboratory in the form of hardware-in-the-loop (HIL) experiments can require high investment costs for infrastructures and might even not be viable in small-scale laboratories. Therefore, system setups for laboratories are presented in this contribution, so that a substantial part of test scenarios is substituted with a simulation in software, forming a combination of software-in-the-loop (SIL) and HIL. Such system setup includes a power interface and measurement system to parallelise the SIL and HIL simulations, and form a so called power hardware in the loop (PHIL). A newly developed system setup for laboratories is proposed to be implemented at HSU and compared with a more common system setup available at AIT. The comparison considers several criteria, such as required components, possible time resolution for the simulation as well as the reaction to a change in the in the simulated system variables (e. g. voltage). Furthermore, the proposed system setup is examined in a holistic test scenario that simulates a real centralised control system, including its ICT systems and the required interfaces, representing a future smart grid. The results show that the proposed system setup offers a sufficient alternative for laboratory tests, especially for smart grid applications that do not require an analysis of transient or dynamic behaviour of the System under Test (SUT).

1 General Information of the User Project

The transition towards renewable energy and decentralized power supply leads to several challenges for the grid operation, particularly on the distribution level. To mitigate potential problems in the power grid, such as voltage violations or over loading, distribution system operators (DSOs) need to undertake smart operation strategies. An example of smart operation strategies the cellular approach is suggested for example in the C/sells [1] and the ELECTRA IRP [2] projects, which divides the grid into smaller cells. Each grid cell tries to solve its own problems based on its own available flexibility, and communicates with other cells to provide or receive flexibility for solving the problems in the entire power system. Such a smart operation and control strategy requires various infrastructure for information and communication technology (ICT) and also various interfaces between the cells as well as between components in one cell.

The Smart Grids Research Group at Ulm University of Applied Sciences (HSU) investigates several grid components and control strategies, especially PV inverters, their control strategies and communication interfaces, considering smart operation strategies for future smart grids (e.g. cellular approach). Such control concepts require the use of ICT combined with control algorithms, which typically have high complexity and thus must be evaluated and analysed extensively in a laboratory environment [3]. Therefore, field tests are usually carried out for such combination before it can become a procedure for the operation of distribution grids or smart grids. However, performing a pure hardware test with only physical components in laboratories for a certain grid cell can require an extensive budget or be even too complex. Hence, a combination of a software and hardware test environment is proposed in this contribution. This proposed test setup is based on a complete simulation of a grid cell in SIL as well as a detailed hardware test of an equipment under test (EUT). Within the SIL test environment, control schemas can be tested and therefore it can be described as a Controller (Hardware)-in-the-Loop (C(H)IL) test. To close the loop of simulation, commands and measurements are exchanged between several components through the ICT systems, which form the ICT-HIL part of the system setup. A Schematic illustration of the main components of the investigated setup is depicted in Figure 1.

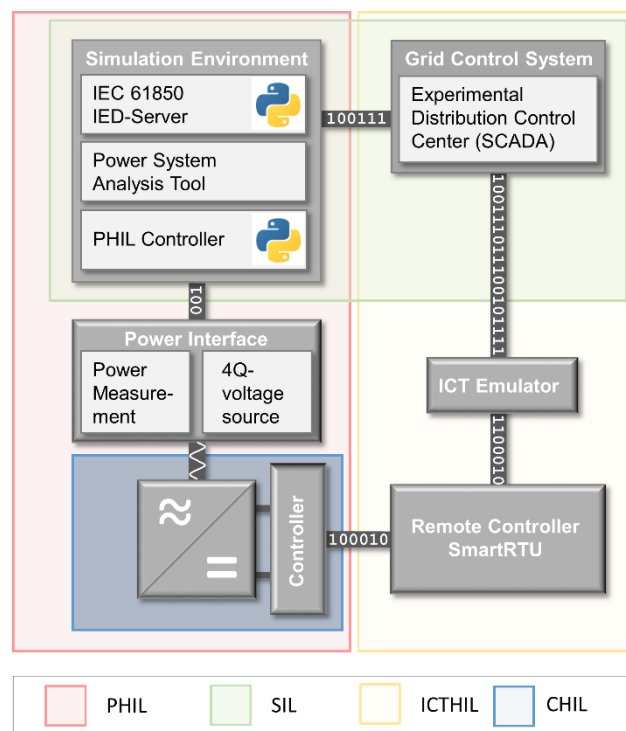


Figure 1: Schematic overview of generic setup for the test and validation of Smart Grid control concepts. Different aspects of the X-in-the-Loop concept are combined or can be used to examine a single topic.

*Research Motivation***2 Research Motivation****2.1 Objectives**

It is planned to utilize a switched-mode power interface (PI), which is available at HSU-laboratory as a key component is for testing complex smart grid systems. This PI is also available at AIT. The primary use of this PI at HSU was system function testing with a given test profile of the voltage, which involves voltage swell, Q(U)-control, etc. It is suggested that this PI can also be used in a PHIL setup, when the main goal is to analyse the overall system behaviour and not to focus on the dynamic behaviour of a single component under test. The systems under the scope of the test environment feature at least one of the characteristics stated in Table 1. Based on the characterisation of the tested systems, the requirements for PHIL setup are stated in the lower part of the table.

Table 1: Requierments for the Setup

Category	Domain	Requirement
Systems Prop- erties	Involved Domains	SGAM Domain: Distribution, Decentralized Energy Resource, Customer Premise
	Communication	communication over WAN (e.g., BPL or Mobil 4G)
	Communication	multiple communication protocols are used and converter
	Control	central and decentralised control
	Control	autonomous or partially autonomous control of multiple systems
	Timing	update and control cycles > 30 s
Requirements	Timing	PHIL cycle time < 1s
	Accuracy	only sinusoidal waveform
	Accuracy	low voltage deviation <1 V _{RMS}

2.2 Scope

Considering the available equipment in the Smart Grid Lab, there is a necessity to combine real time simulation with HIL tests in order to perform the planned tests. Given the opportunity provided by ERIGrid Transnational Access, a diversity of equipment and possible setups are available at AIT, so that the targeted setups can be realized and validated. In addition, the experience and know-how by both AIT and HSU, which was accumulated over years through performing many lab experiments, can be exchanged and further developed.

3 State-of-the-Art

For the laboratory testing, one seeks for an environment with a variety of parameters to control. This setup can be described with the term of real-time hardware-in-the-loop (HIL) concepts [4]. The basic idea behind it is to place a system in an environment in which all inputs and outputs can be controlled. For the testing of power system components an additional key interface is necessary which is the Power Interface (PI), as it can provide voltages in the typical range of a power hardware [5]. Besides, there are further domains which can be simulated and controlled relevant for the holistic system testing of a smart grid strategy. They are listed and explained in Table 2.

In general terms, this means that a test candidate (system, component or algorithm) is placed in an environment, where the adjacent systems are simulated, and the behaviour at the points of interface is emulated. Figure 2 depicts this approach in a generic way. Based on the reaction of the system-under-test (SUT), the simulated environment is adapted accordingly.

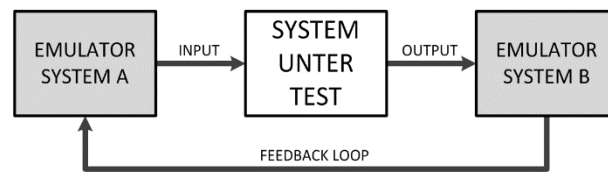


Figure 2: Generic setup of a X-in-the-loop as a concept for system testing

Table 2: Comparison of different domains using the X-in-the-loop concept for system testing with the focus on the energy sector

Name	Description	Ref.
Hardware-in-the-Loop (HIL)	The subject of the system testing can be any physical component which is able to provide small scale input and output signals. HIL can also be seen as general term and can be specified by the following test categories	[6, 7]
Software-in-the-Loop (SIL)	Software components are the subject of a SIL test setup. The input and output signals are calls and responses of the adjacent software components which are emulated.	[8]
Controller Hardware-in-the-Loop (CHIL)	Subject are the controller boards of a power hardware device. A CHIL setup will therefore simulate the mechanical, electrical and power electronic parts of the power hardware device, which are controlled by the tested controller board. In contrast to a PHIL-setup, the controller board is introduced to the small signals which are typically provided by the power hardware. The reaction of the controller board to a disturbance can be examined and resulting voltages and currents can be evaluated regarding the relevant specification. CHIL tests are typically undertaken before lab testing of the complete device.	[7]
Power Hardware-in-the-Loop (PHIL)	The subject of this system is a component from the power system domain. In contrast to HIL, the input and output signals can be typical power systems levels, e.g. a common low-voltage connection with 400 V _{AC} and up to a nominal power of 1 MVA	[4, 6, 7]
ICT Hardware-in-the-Loop (IC-THIL)	A complex smart grid system is typically based on communication and relies on package-based communication connection like IP/TCP or UDP, which often suffers from impairments like latency, package drop, package reorder or corruption of data in real-world applications. This means, when testing a system these effects have to be reproduced as well. Therefore it is e.g. necessary to precisely weaken the transmission path. This effect can be achieved by using a physical network emulator. If the communication network is simulated as well, the term Network-Simulation-in-the-Loop (NSIL) can be used	[8–10]

4 Executed Tests and Experiments

This contribution focuses on two system setups, which can be used to evaluate the performance of smart grid components as well as validate new solutions for smart grids with high renewable energy feed-in. In the first phase, the proposed system setups are tested and compared in the proposed simulation scenarios. In the second phase, the target system setup is tested and evaluated in a smart grid simulation environment, considering the complexity of real grid operation.

4.1 Test Plan

The examination of both used system setups is carried out by comparing the response of the systems within three different scenarios. These are:

- **Step Function:** Voltage deviation at the slack bus bar from 1.04 p.u. to 1.08 p.u. in a step. This represents the most extreme change of a parameter in the modelled system. It has been chosen to evaluate the difference in the dynamic behaviour of the systems in the time domain of seconds.
- **Transient Behaviour of the Step Function:** The voltage change of the two setups is evaluated regarding the transient behaviour of the system.
- **Ramp Function:** Voltage deviation at the slack bus bar from 1.04 p.u. to 1.08 p.u. as a voltage ramp over the course of 1 to 10 minutes. These are typical changes which can be deployed to examine the stability of systems in varying conditions.

The individually used experiments are depicted in Figure 3 which also shows the system setups and the used grid model. The depicted experiments are grouped into three parts. These are the previously described tests for the comparison which are called Phase 1. Phase 1 is accompanied with a preliminary test to characterise the system setups which is referred to as Phase 0. The subsequent tests are subject to a case study which is called Phase 2. These tests have been executed within the ERIGrid TA project "Smart beats Copper" at the host facility AIT in Vienna, Austria, as well. Additional tests with system setup B have been executed at the Smart Grid Lab of Ulm University of Applied Sciences, Ulm, Germany.

In order to examine the performance of the developed systems, two simulation scenarios will be applied. In the first scenario, a voltage increase in single steps is implemented by means of increasing the set voltage in the slack bus bar. Such a scenario of voltage increase can be observed in practice, if a regional transformer changes the position of its On-Load Tap Changer (OLTC). In the second scenario, a gradual voltage increase in a ramp is implemented by means of increasing the set voltage in the slack bus bar. Such a scenario can be observed in practice if voltages in the medium voltage grid increase according to natural increase of PV feed-in during a clear sky day.

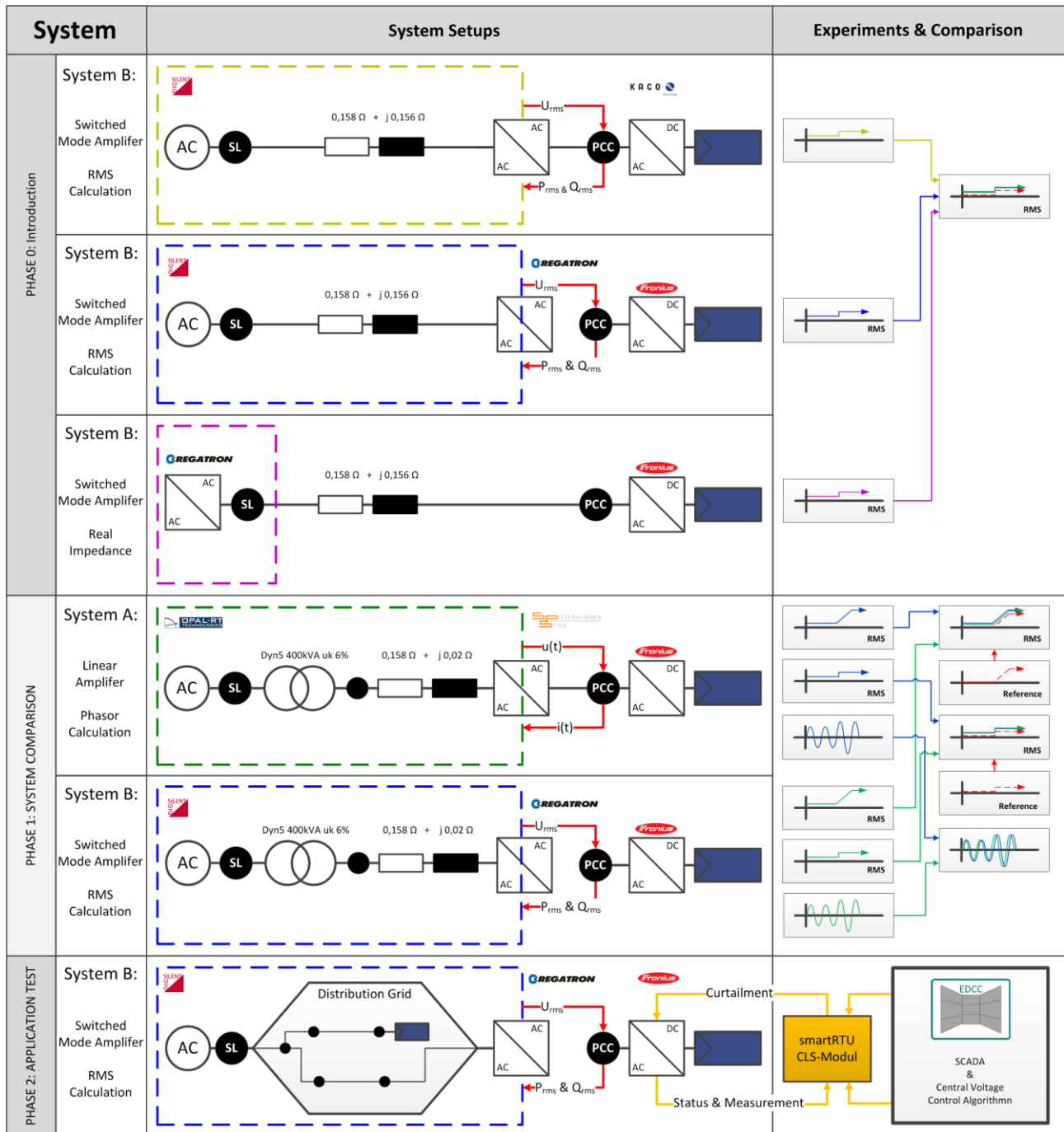


Figure 3: Schematic overview of the test scenarios for the comparison of the system response which is split in three phases. The system setups and the implemented grid models as well as the individual experiments and the carried comparisons are shown. The colour of dashed box corresponds with the graphs in the following section.

4.2 Case Study

This experiment was the main example use case when designing the comparison of the previous section. Therefore, the actual process of setting up and carrying out this experiment is described hereinafter. The scope of the contribution is therefore widened and enriched with real results. Moreover, finding a flawless control algorithm was not the aim of the carried-out experiment. The chosen algorithm is not suitable for this application but shows the necessity of the complete testing procedure.

- **System under Test:** The purpose of this case study experiment is to observe the performance

and reaction of the EUT responding to smart grid control strategies in a controlled environment. In this case the EUT is a Fronius PV inverter with its active power feed-in regulated by a coordinated voltage control strategy. The inverter has a nominal active power of 20 kW, due to active power restriction, the nominal value is limited to 10 kW during the experiment. The Q(U) setting applied to the EUT is the same as in Phase 1. To distinguish the EUT from the SUT, the SGAM layer representation in Figure 4 can be used. The SUT can be identified as the complete construction shown in the diagram which consists of a Supervisory Control and Data Acquisition (SCADA) system, a fleet management for the smartRTUs (also referred to as CLS Management), traditional RTUs and smartRTUs and the depicted primary equipments.

- **Communication and Control Infrastructure:** The control infrastructure consists of several essential hardware and software kits. These include a site controller as active power regulator, an experimental distribution control center (EDCC) as grid control system, a controllable local system (CLS) management as secured data transfer interface and a virtual station controller as interlinking between power interface and simulation environment.
The site controller, also widely known as a CLS-box, is part of the basic components of the smart metering infrastructure in Germany, which is described in detail in the Technical Guideline TR-03109-1 [11]. The CLS-box fulfills the role of a site controller by monitoring and controlling the PV inverter via SunSpec protocol compliant communication. At the same time, the CLS-box acts as an IED Server (i.e., IEC 61850 Intelligent Electronic Device [12]) and transmits power measurements of the PV inverter, which are defined by the power interface via an encrypted channel, to the CLS Management Server. The site measurement data are ready to be subscribed by IED Clients through a secured channel. In this case study, the IED client is the EDCC at Ulm University of Applied Sciences, where a grid control system including SCADA of the type SPECTRUM POWER 5 by Siemens.

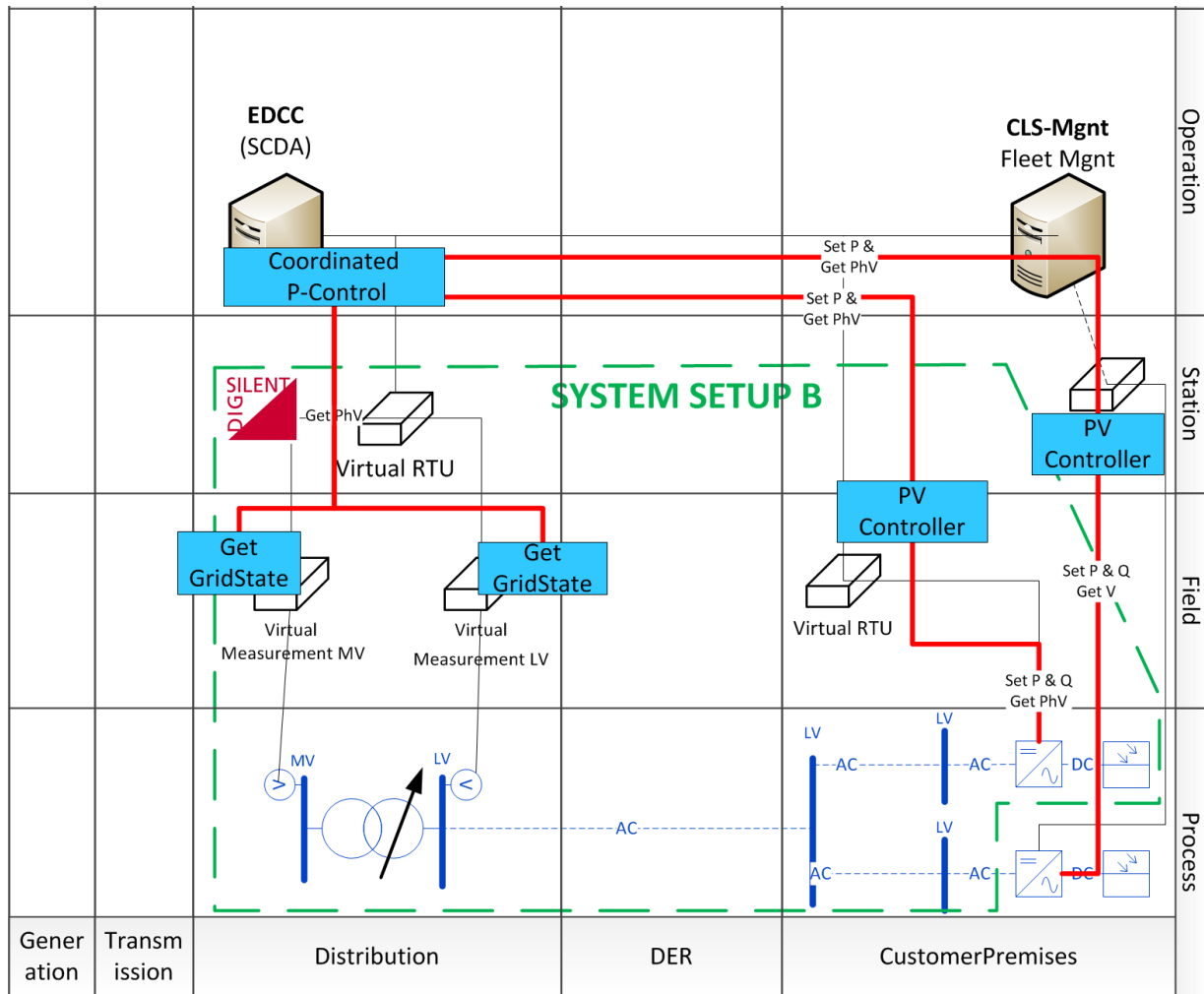


Figure 4: Combined SGAM-layer-diagram of the implemented case study. The base layer depicts the real and the simulated components as well. The boundary of the PHIL setup is illustrated as a green dashed line. The utilized functions are depicted in blue boxes.

4.3 Test Set-up(s)

4.3.1

The investigated system setups are described in details hereinafter.

System Setup A

The system analysed first is based on a linear signal amplifier (i.e., Spitzenberger Spies PAS [13]) as power interface which simulates a grid connection point from the simulated grid. The PI receives an analogue voltage signal from the DRTS (i.e., Opal-RT [14]), which generates the signal according to the parameters of the simulated grid connection point (e.g., voltage U_{pcc}). These parameters are calculated within a real-time dynamic simulation with a high-time resolution of typically 10-50 μs , based on a code-generated model converted from a MATLAB/Simulink model. To close the simulation loop, the DRTS is fed back with analogue current measurements, which are converted internally to digital values to be entered into the simulation model. These transient measurements correspond to the feed-in power of the PV inverter (i.e., EUT: Fronius PV inverter [15]), which is connected physically to the power interface representing the Point of Common Coupling (PCC) of the grid. For the purpose of recording the simulation results, an external measurement system will be connected to the PCC (c.p. [16]). The described system is illustrated schematically in Figure 5 along with the second setup which is discussed in the following section. In the course of the following sections this setup will be referred to as System Setup A.

System Setup B

This setup proposes the utilisation of the steady-state load flow calculation of the power system analysis software (i.e., DlgSILENT PowerFactory [17]). The calculated voltage value at a predefined bus bar in PowerFactory is passed as a new voltage set point to a PI, which in this case is a switched-mode voltage source from Regatron (i.e., Type: TC.ACS [18]). For sending the set values, an interface is programmed in C# language which utilises the API provided by the manufacturer to communicate with PI.

A PV inverter (cp. [15]) is connected physically to the voltage source as EUT and feeds in power to the grid. The active and reactive power of the PV inverter is captured by a measurement device (cp. Janitza UMG96 [19]). The RMS measurements are fed back to the simulation in PowerFactory as digital values to form a closed loop. For this measurement feedback, an interface is programmed in Python utilising Modbus/TCP functionality of the measurement device.

The system setup is illustrated schematically in Figure 5. In order to control the voltage in the simulation of PowerFactory, an external function is programmed in Python. In order to control the voltage in the steady state load flow calculations of PowerFactory, another external Python function is developed for the control and synchronisation of these calculations. In the course of the following sections this setup will be referred to as System Setup B.

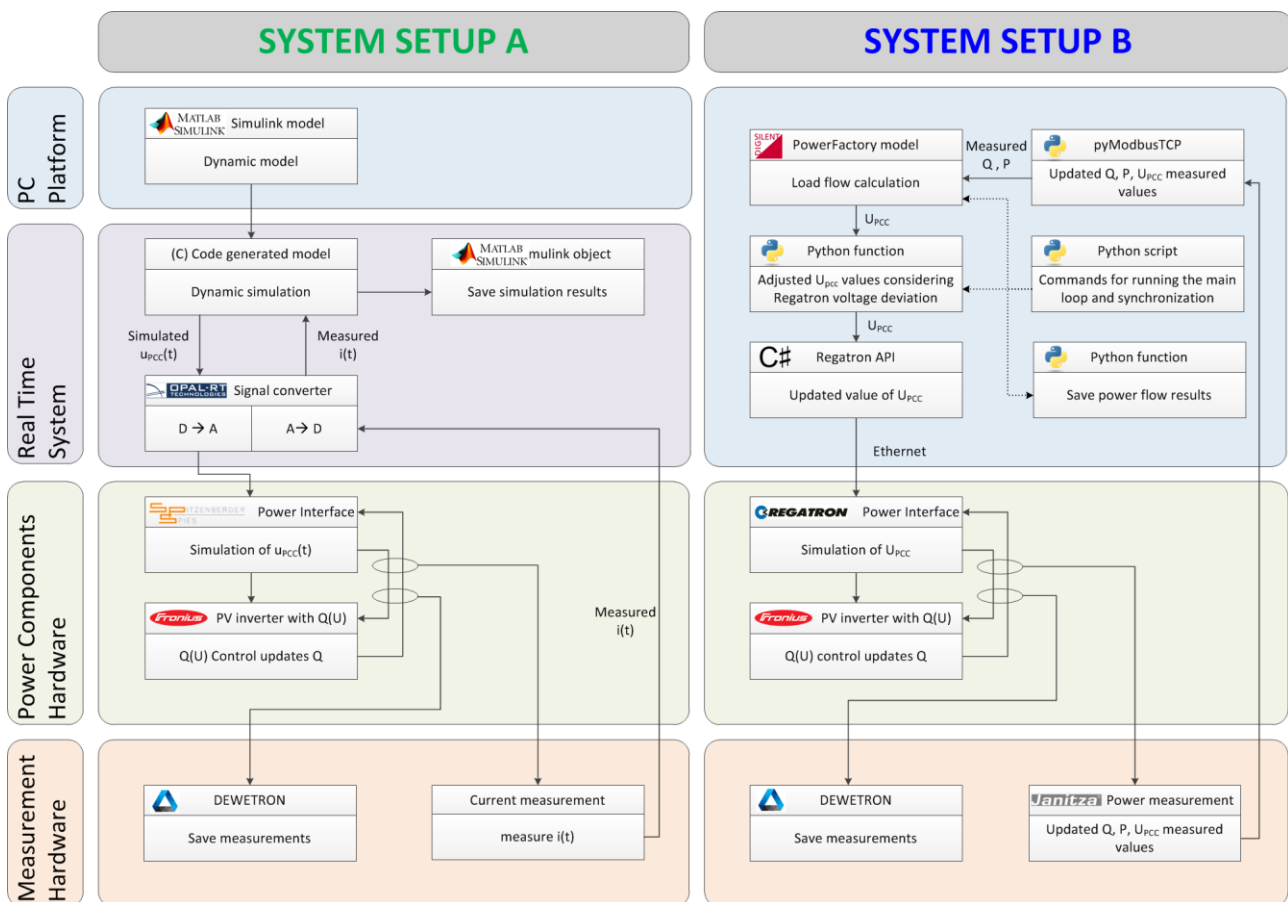


Figure 5: Comparison of the architecture of the used system setups: System Setup A – Opal-RT RT-LAB based system with Spitzenberger Spies PAS. System Setup B – Digsilent PowerFactory based system with Regatron TC.ACS.

Monitoring

The monitoring of the carried out experiments is done by the utilisation of the independent measurements device of the type Detwetron DEW-800 [16] with the corresponding voltage transducers/amplifiers for the corresponding voltage levels. In addition, the measurements through Janitza UMG96 [19] of the System Setups B as well as the simulated values are recorded as well.

4.3.3 Control Strategy for Case Study

The virtual IED Server transmits the grid information via Virtual Private Network (VPN) to the EDCC, where a voltage control algorithm is implemented and configured as a visual basic script. As a result of interacted hardware measurement and software simulation, a power curtailment setpoint, represented as a percentage value with respect to nominal active power, was sent back to the CLS-box and was subsequently forwarded to the PV inverter. The voltage regulation would be triggered when the voltage was bigger than 1.05 p.u. The active power curtailment was transmitted to the inverter in gradual steps by 10% exceeded 0.05 p.u. The used control algorithm can be described by the following equation:

$$P_{Limit} = P_{nominal} * f_{curtailment}(U_{PCC}) \begin{cases} f = 0.0 & U_{PCC} \geq 1.080 \text{ p.u.} \\ f = 0.1 & U_{PCC} \geq 1.075 \text{ p.u.} \\ \vdots & \\ f = 0.9 & U_{PCC} \geq 1.055 \text{ p.u.} \\ f = 1.0 & U_{PCC} \leq 1.050 \text{ p.u.} \end{cases}$$

4.4 Data Management and Processing

The main source for measurement data was the independent measurement device, which was not involved in the experiment other than for observation. The measured data was stored in the manufacturers proprietary file format (.d7d-files). A file naming convention was implemented to keep track of the experiments and measurements files as well the auxiliary files, like reports and logs of the different involved software tools, which were part of the experiment.

As the measured signals were captured at a rate of 20 kHz, it is possible to extract calculated values at any given time after the experiment. This feature was used to obtain 1 period RMS for the further analysis and save these measurements as a .csv-file. The visualization and calculation of the statistical key figures are made with the data mining framework KNIME [20]. For the publication ready plotting the python library matplotlib is used. This process is shown in Figure 6.

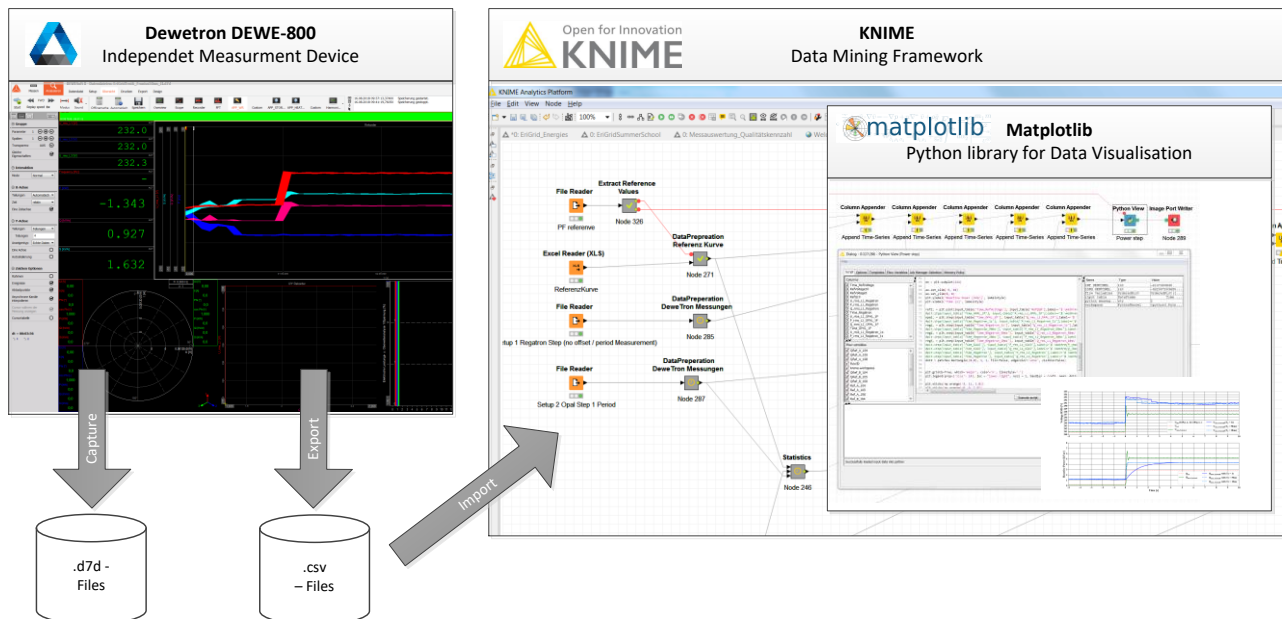


Figure 6: Used Data Management Tool Chain and Processing for the Experiments. Measurement are taken with the independent measurement device and stored in the proprietary file format. The derived data is imported by the Data Mining Toolbox KNIME via a .csv-file. For publication ready graphs the python library "matplotlib" is used.

5 Results and Conclusions

5.1 Comparison of the transient behaviour of the system setups

This section focuses on the comparison of the two setups described in Section 4.3. At first, the comparison of the used systems is made by analysing their transient behaviour. The trend of the voltage and the current of the two 3-phase systems are depicted in Figure 7, respectively Figure 8. Both systems changed from one given waveform, which corresponded to a value of 240.6 V_{RMS} , to another waveform with a corresponding value of 249.7 V_{RMS} within roughly 100 microseconds, respectively 232.9 V_{RMS} to 241.3 V_{RMS} . For both systems no lasting disturbance in waveform of the voltage could be observed. The given ideal sinusoidal waveform for the voltage was generated by both systems with neglectable fractions of no fundamental parts. The capabilities of both systems to generate a varying amount of non-fundamental disturbance have not been examined further in this contribution.

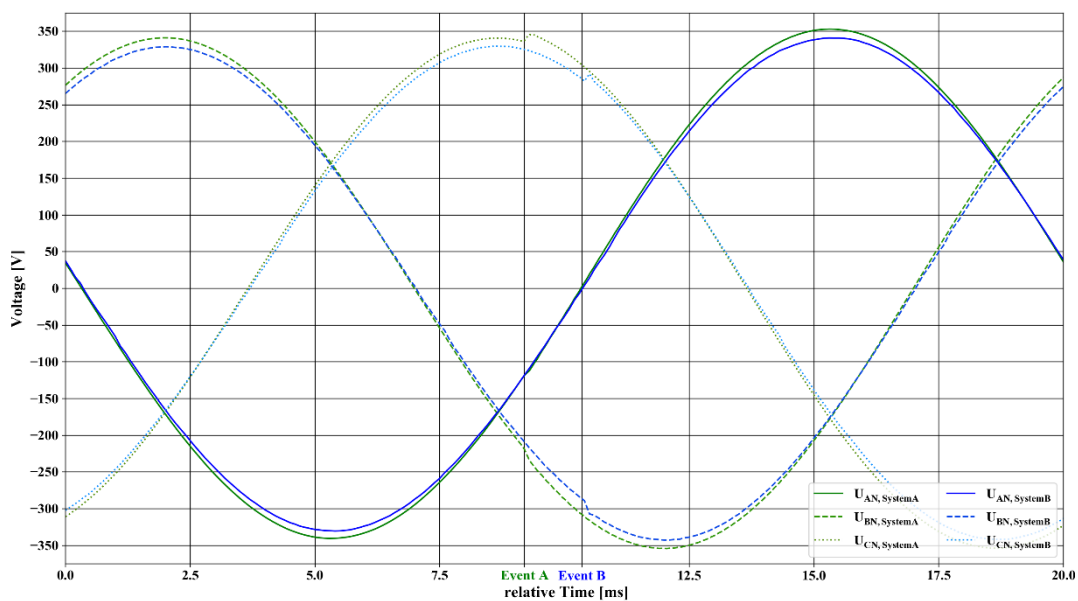


Figure 7: Comparison of the different transient system responses to the step for the current feed-in by the PV inverter. The currents of both 3 phase systems are overlayed and synchronized. The occurrence of the step event is indicated separately for each setup.

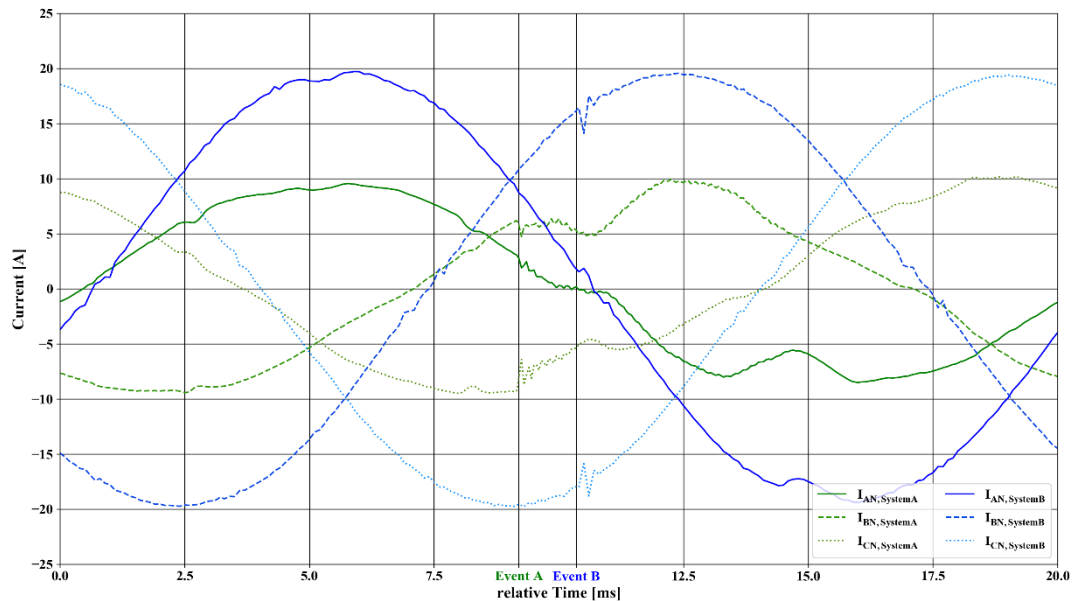


Figure 8: Comparison of the different transient systems response to the step of the voltage. The voltage of both 3 phase systems are overlayed and synchronized. The occurrence of every step event is indicated for each setup separately. Neither system shows a significant amount of disturbance

5.2 Comparison of the system behaviour to a voltage step

The evaluation depicted in Figure 9 focuses on the dynamic behaviour of the systems for the test scenario. This change of perspective also can be understood as change from the evaluation of the individual power interface to the evaluation of the complete PHIL setup. The 1-period RMS values provided by the independent measurement device have been used for this evaluation.

As a reference, the steady state values for the used grid model and implemented Q(U)-control are the parameters for the constructed curve which is plotted as a red dashed line.

The experiments have been carried out in individual runs. This means that the measured curves are aligned with the ideal step function. Therefore an offset between the parameterised step and the actual step cannot be observed in the graphs. This offset was limited to a maximum of one simulation step. For System Setup B this was limited to a maximum of 420 ms.

Three interesting aspects could be observed regarding the step functions: (i) the voltage deviation for the steady state situations before and after the step, (ii) the constancy of selected setpoints and the overall stabilisation time. In addition, (iii) the stabilisation time is highly affected by the implemented control algorithm (e.g., Q(U) control) and the selected parameters.

The varying time constants of the Q(U) control could be observed when looking at the different responses of the PV inverter to the voltage step. For System Setups A and B, the inverter reacted immediately with a small time constant with a reactive power in-feed when the voltage changed. Smaller time constants resulted in faster reach of a steady state. For both setups, the reaction of the inverter was immediate when small time constants were used. In contrast to that was the calculated reaction to the changed reactive power in-feed by the system setups. For System Setup A the reaction of the voltage happened immediately due to small time steps of the PHIL-setup, whereas for System Setup B the reaction was delayed in more discrete steps which corresponds to the cycle time. The time constant suggested by the manufacturer is $T_C = 5\text{s}$ which will result in a highly damped system response. This seems to be a preferred strategy for DSO to prevent interference with multiply deployed systems.

The upper dashed line represents the 1.08 p.u. value and, as one can see, the voltage of system setup B never dropped below this parameterised limit of the Q(U) control. According to the given droop curve of the Q(U) controller this resulted in a constant reactive power.

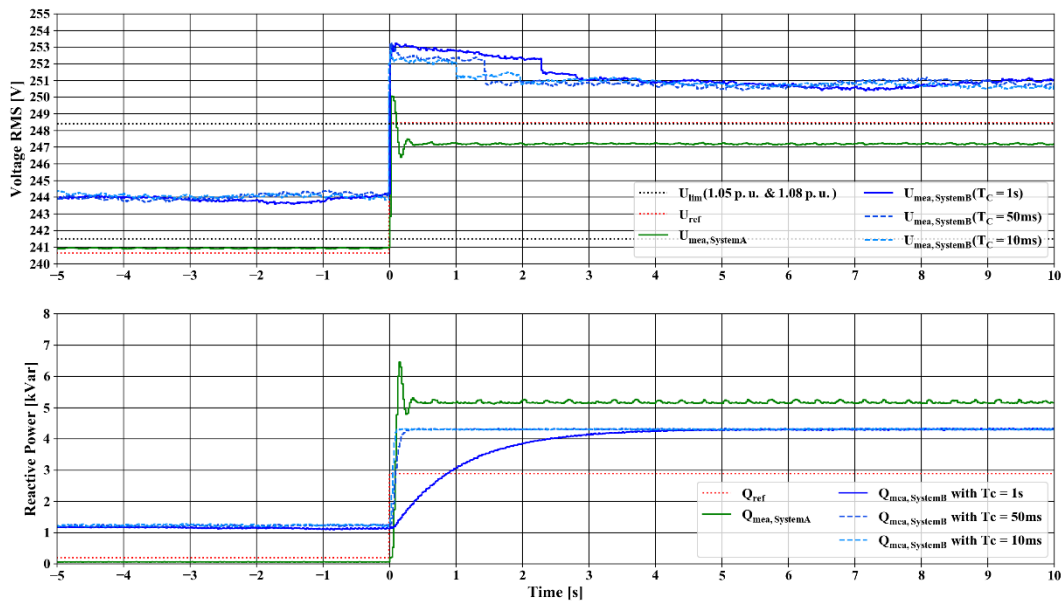


Figure 9: Comparison of the different system responses to the deviation voltage step. The reference curve is constructed by using the steady state results for given Q(U)-control. For system setup B varying time constants T_c for the Q(U) controller of PV inverter are presented. The depicted values are RMS-values calculated on a 1 period time frame. The dashed line represents the values for 1.05 p.u. as well as 1.08 p.u. which in turn are the setpoints for the break of the slope of the Q(U) controller.

5.3 Comparison of the system behaviour to a voltage ramp

In comparison to the previous section where the focus lay on the comparison of the two systems in regard to the transient and dynamic behaviour when changing the voltage in an extreme manner, this section compares both systems in the context of a slowly but constantly rising voltage level and the interaction of the Q(U) control. The results of this comparison are shown in Figure 10. In contrast to the short term evaluation of the step function this test scenario was executed with a variety of durations with up to 10 minutes of rise time. The scenario with a rise time of 10 minutes is outlined in the current section. To evaluate this rather long-term scenario, two different active power levels have been chosen. This is due to the system properties of system setup A, as the complete feed-in energy was dissipated by the PI. In the course of the experiment issues regarding the overheating and thermal shutdown had to be tackled.

The reference curves for the ramp illustrate what is expected in theory. The red dashed line represents the constantly raising voltage level of the upstream grid with the inverter working against the voltage raise with feeding-in reactive power. When comparing the measured values, both systems showed a voltage deviation from the calculated value. For System Setup B this deviation lay within the same order as it already could have been observed in the step experiment. With system setup A the voltage changed from over-voltage in respect to the reference curve to under-voltage due to a higher reactive power infeed. The individual oscillation appeared in the same order of magnitude as in the previous scenario. The reactive power response of System Setup B became in the bigger time frame of this analysis quite pleasing. For System Setup A the reactive in-feed was too high due to a different parameterisation.

The active in-feed power remained constant for both setups. The vertical line which is annotated with 'Event A' represents the point where the power interface of system setup A shuts down due to over-temperature.

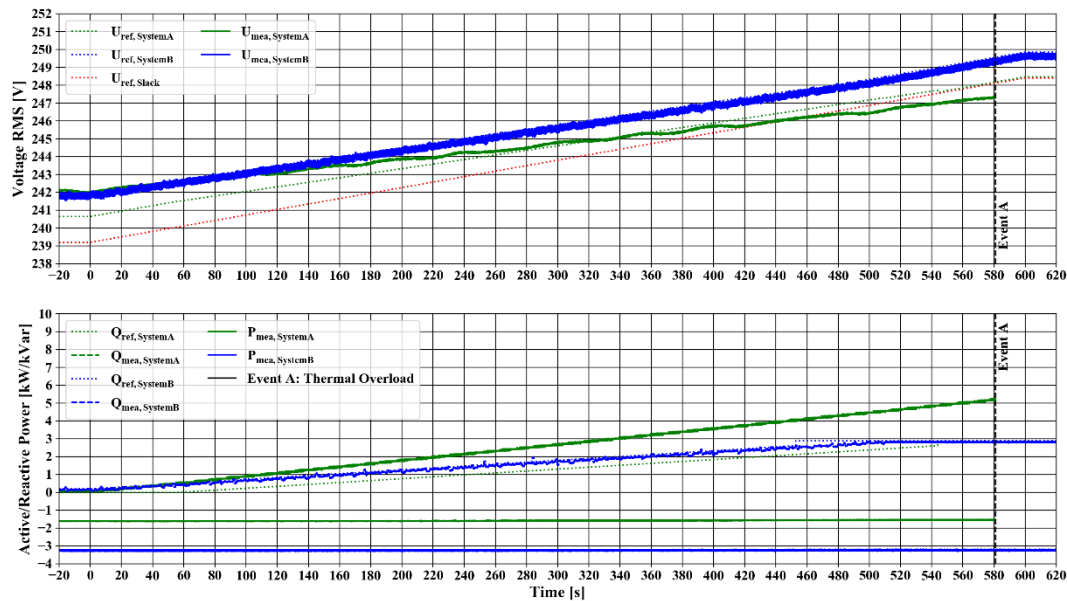


Figure 10: Comparison of the different system responses to the deviation voltage ramp with the raise from 1.04 to 1.08 p.u. at the slack node over the course of 10 minutes. The thermal overload of the PI of system setup A is indicated.

5.4 Case Study: Overlayed Voltage Control Algorithm

The described methodology was used to test and evaluate the setup described in Section 4.2. The simulated OLTC of the grid was actuated to step through the voltage range and to trigger the two Q(U) & P(U) control regimes. Figure 11 shows the results of the executed experiment as a plot of active, respectively reactive power over the voltage at the PCC of the inverter. The described steps can be seen in clusters of data points in the diagram. The characteristics for the local Q(U) and the superior P(U) control are represented as lines as well. The green coloured area represents the anticipated deviation for the Q(U) control due to output filters and error of the measurements from the inverter as well as from the independent measurement. Nevertheless, the measured values for Q(U) control remain close to the desired characteristics. Looking at the P(U) control governed by the SCADA system it can be noticed that: The deactivated P(U) control results in stable operating points at different set points of the simulated voltage regulator of the transformer. The in-feed power of the inverter is not curtailed. With activated P(U) control, the purple coloured area represents the undesired voltage range. As the control-algorithm is a very basic lookup-table, the voltage has to be within this area for at least one transmitted period.

In the active power and voltage plot in Figure 11, a few control actions of the control algorithm are depicted. The value pairs form four main clusters, which are inherent to the used setup. The direct causes of the change from one cluster to another are described in the following list:

- (A → B) Voltage within the undesired range. Also curtailment command is transmitted after the executed cycle of the control algorithm. Decrease in feed-in power due to the curtailment command, and slightly reduced voltage level due to the inherent properties of the voltage source (please refer to the previous section).
- (B → C) Due to a new voltage set point for voltage source the voltage readings decrease after a load flow calculation is carried out.
- (C → D) With the next performance of the tested control algorithm the voltage is in an acceptable range, and the curtailment is retracted. Due to the inherent properties of the voltage source the voltage increases slightly.
- (D → A) With the next carried out load flow calculation the system state returns to A.

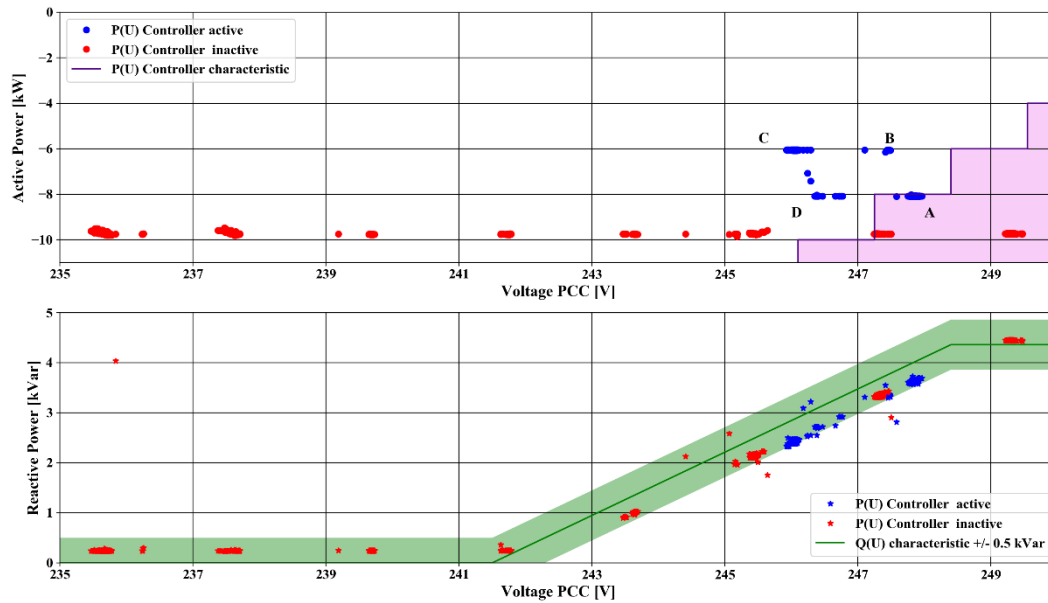


Figure 11: Comparison of the coordinated $P(U)$ control governed by the EDCC and the $Q(U)$ control of the inverter. Control characteristics are represented by the purple, respectively green lines

The analysis showed that the proposed setup with a simple test algorithm is working. This is visualized in the time-series plot of Figure 12, where the measurements of the independent measurement device and the transmitted readings of the SCADA system are compared. Due to the automatically sent commands of the SCADA system, the field gateway is passing the curtailment to the inverter. The inverter is limiting the feed-in to the desired value. This leads to a change in voltage level due to the PHIL setup. As result of the experiment, the postulated oscillation is occurring, nonetheless the control algorithm would not be suitable for a real grid operation. When comparing the measurement and the transmitted values of the SCADA system, the discretisation evoked by the technical constraints is clearly observable.

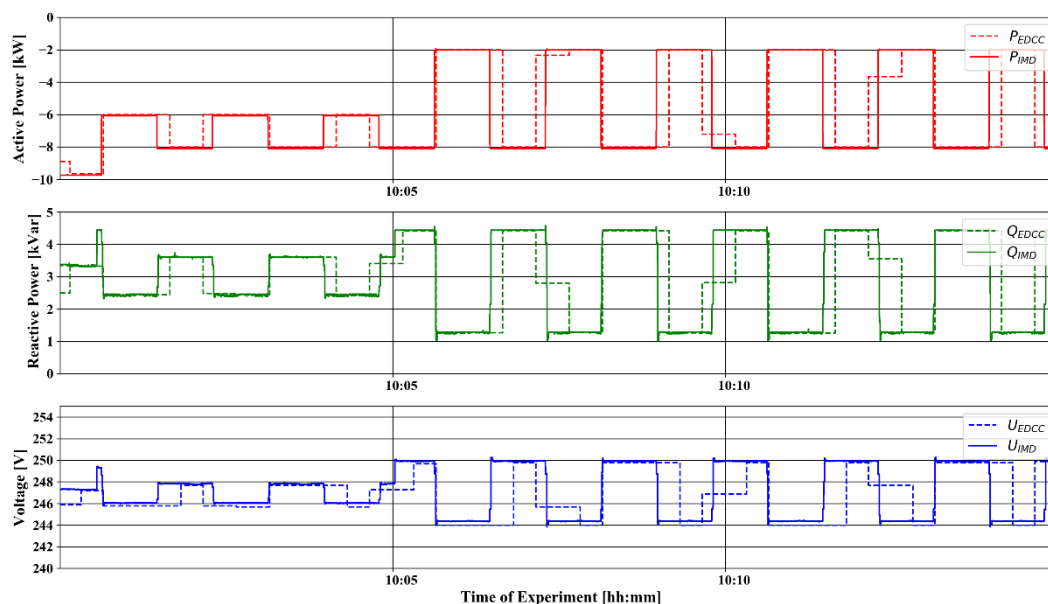


Figure 12: Transmitted Readings (EDCC) and independent measurements (IMD) for a time period with activated $P(U)$ control algorithm.

5.5 Evaluation of the cycle time of System Setup B

System Setup A was able to meet the time requirements due to its real-time control loop with a cycle time well below $50\ \mu\text{s}$. For System Setup B, the cycle time was significantly higher and required a more detailed analysis. As shown in Figure 13, the total cycle time remained under one second. The cycle time t_{PHIL} for System Setup B consisted of the control loop in the main loop, the calculation of the new setpoints in PowerFactory, the control of the switched-mode amplifier and the feedback of the measured values. The main control algorithm was implemented as a python script, which took about 20-30 ms runtime. Although the underlying interpreter required a bit more time to execute than a compiled program, new interfaces can be quickly and flexibly integrated into the process using Python. This also applies to PowerFactory, which is controlled by a dedicated Python interface. Due to the simple grid model, the load flow calculation including feedback took 50 ms (+/- 5). The feedback contained the new setpoint for the switched mode amplifier. Its manufacturer provides a C# library with which the new setpoint value can be communicated to the device via Ethernet. The time needed to execute the command could not be further optimised and lies at 250 ms (+/- 50). To access the C# interface, a helper application was used, which is coupled to the python main loop via a named pipe. Subsequently, a new actual value was queried by Modbus/TCP from the measuring device and thus the control loop started again. This last step required 100ms (+/-20). Overall, a t_{PHIL} with a median of 420 ms could be achieved with System Setup B. The cycle time shown for different experiments is depicted as violin plot in Figure 13. The density representation shows 2 respectively 3 clusters for the cycle time with the highest density around the median. The second cluster is in range of 0.2 s to 0.3 s. Due to the added IEC61850 simulator function used in the case study this cluster is moved towards the median.

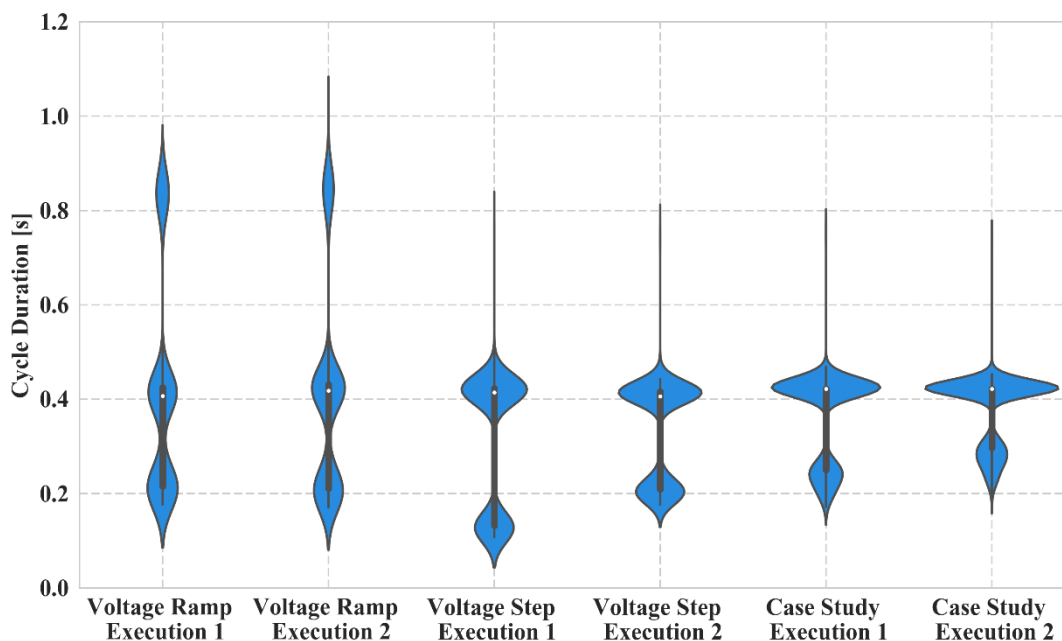


Figure 13: Illustration of the cycle time t_{PHIL} for system setup B for use in the evaluations of Phase 1 as well as for use in Phase 2. The white circle represents the median of the violin plot, the bold line represent the interquartile range and a density representation.

5.6 Conclusions

System Setup A and System Setup B have been able to provide 3 phase voltage systems, which are suitable to synchronise the given PV inverters, and started to operate properly. The modelled grid was used for a load flow calculation, and the extracted voltage signal was forwarded to the power interface. The Q(U)-function of the inverter has been tested as well. The biggest draw back

observed in the carried out experiments has been the significant voltage deviation for System Setup B. Based on further examinations, we assume that the offset has been caused by an immanent impedance. In these examinations a proportional offset from the idle state voltage setpoint to the idle state voltage present at the terminals of the power interface occurred. When changing the consumed or feeding power independent of voltage set point, the voltage offset changed as well. Therefore it is expected that the offset could be compensated with simple correction equations, which do not even introduce another controller to the system. Alternatively, the PI of System Setup B could be replaced with a superior PI of System Setup A, which featured a lower impedance and would therefore have reduced the undesired effects. Nonetheless the dynamic properties would stay the same.

The occurred automatic power shut-off to prevent overheating of the PI of System Setup A could be tackled by using an additional load to prevent the feed-in energy being dissipated within the PI. This would also alter the Thevenin-equivalent of the setup which might be undesirable. Regarding the quality of the provided voltage signals, both systems generated negligible amounts of harmonics. To represent real grid situations, it has to be considered to introduce a realistic amount of harmonics.

Regarding the soft facts, involving setup and training, System Setup B seemed less challenging as the options were more limited. As an addition, the software PowerFactory is one of the standard tools used at HSU not only for real-time simulation but also for scenario and time series analysis of distribution grids. Using those models and calculation algorithms in pure simulation experiments and in PHIL testing is beneficial. The models had to be setup up only once and results from the simulation were helpful in the PHIL experiment design. In addition, the results from the PHIL experiment could improve the models implemented in the simulation environment.

Another difference between the PI of the two setups was the maximal frequency at which the systems could reproduce harmonics. For system setup A, this was limited to 30 kHz whereas for system setup B, this was limited to 5 kHz. This aspect was not a prominent requirement for the contemplated usage.

As a conclusion it can be stated that there was a significant difference in the working principle of the two system setups. Both systems could provide a function essential for the evaluation of EUT and SUT. System Setup A was more accurate and showed more capabilities than System Setup B but this came to the price of a more complex system regarding modelling, setup and operation than it was required in System Setup B. In addition, the expenditures for purchase and maintenance have been higher for System Setup A compared to System Setup B. Regarding the use of electric energy, the PI of System Setup B was able to feed back into the grid, whereas the linear PI of Systems Setup A dissipated the energy.

As a result, different levels of accuracy and continuity of the output signal have been observed. The difference of the systems are apparent for the reaction of the Q(U) controller of the PV inverter within the test environment. If the time constant of the Q(U) controller is significantly lower than the cycle time, System Setup B shows discrete steps of the voltage and the stabilization time is prolonged. As an overall statement, the presented System Setup B is suitable for the use case described. One issue which occurred during the test was an offset between the set-point sent to the PI and the actual voltage measured at the terminals. It is suspected that this problem is caused by the high immanent impedance of System Setup B. This problem needs to be tackled.

In the second part of this contribution, an actual utilisation of System setup B is presented, which shows the intended use for a combined PHIL and SIL testing of complex smart grid control functions. The use of the SGAM presentation provided a basis for a common understanding of the presented test. This is in line with the holistic testing description introduced by the ERIGrid Consortium. Due to the description of the planned scenario, the different facilities were able to implement sub-functions in an efficient manner and were able to test the relevant sub-functions before the actual experiment. As the outcome of this case study the tested central control algorithm is not useful for actual grid operation, as it was anticipated and deliberately chosen at the stage of test design. But the gathered data provided a good basis for the validation of the process.

In addition, the carried out experiment is a successful pilot test for the application of the CLS-Modul. It showed clearly that gathering of relevant measured values at the grid connection point and the generation unit is possible with the implemented SunSpec to the IEC 61850 converter. The other way round was tested as well and the curtailment of the PV inverter was successfully carried out.

6 Open Issues and Suggestions for Improvements

As further steps, the System Setup B will be improved to solve the issues regarding the occurring offset without the use of an additional controller. As first evaluations suggest the effects are fairly linear and are likely caused by a high immanent impedance of the PI. Therefore, further analyses and engineering will be necessary. These will also include considerations regarding the implementation of the immanent impedance in the grid model. The implemented System Setup B is and will be used at the Ulm University of Applied Science in the course of different research projects. The setup will be mainly used for pilot testing of applications involving small decentralised control units in combination with the German Smart Meter Infrastructure which consist of the combination of Smart Meter, Smart Meter Gateway and CLS-Module to enable information gathering and control of small generation units like PV inverters as tested in the case study. These measurements are necessary in preparation of a broader deployment in the demonstration project C/sells [1].

7 Dissemination Planning

Journals:

Comparison of Power Hardware-in-the-Loop Approaches for the Testing of Smart Grid Controls, Ebe F.; Idlbi, B.; Casel, M.; Kondzialka, C.; Chen, S.; Heilscher, G.; Seitzl, C.; Bründlinger, R.; Strasser, T. A. - MDPI Energies - Special Issue: (in Press)

Conferences:

An approach for validating and testing micro grid and cell-based control concepts - Ebe F.; Idlbi, B.; Casel, M.; Kondzialka, C.; Chen, S.; Morris, J.; Heilscher, G.; Seitzl, C.; Bründlinger, R.; Strasser, T. A. - Proceedings of the CIRED Workshop 2018- 7/8.06.2018 - Ljubljana - Slovenia

Presentation:

Comparison of Power Hardware-in-the-Loop Approaches for the Testing of Smart Grid Controls – Falko Ebe - IRED side-event “Laboratory-Based Methods for Smart Grids”- 16.10.2018 - Vienna - Austria

8 Annex

8.1 List of Figures

Figure 1: Schematic overview of generic setup for the test and validation of Smart Grid control concepts. Different aspects of the X-in-the-Loop concept are combined or can be used to examine a single topic. Research Motivation	7
Figure 2: Generic setup of a X-in-the-loop as a concept for system testing	9
Figure 3: Schematic overview of the test scenarios for the comparison of the system response which is split in three phases. The system setups and the implemented grid models as well as the individual experiments and the carried comparisons are shown. The colour of dashed box corresponds with the graphs in the following section.....	11
Figure 4: Combined SGAM-layer-diagram of the implemented case study. The base layer depicts the real and the simulated components as well. The boundary of the PHIL setup is illustrated as a green dashed line. The utilized functions are depicted in blue boxes.	13
Figure 5: Comparison of the architecture of the used system setups: System Setup A – Opal-RT RT-LAB based system with Spitzenberger Spies PAS. System Setup B – Digsilent PowerFactory based system with Regatron TC.ACS.	14
Figure 6: Used Data Mangement Tool Chain and Processing for the Experiments. Measurement are taken with the independent measurment device and stored in the porparitary file format. The derived data is imported by the Data Mining Toolbox KNIME via a .csv-file. For publication ready graphs the python library “matplotlib” is used.	16
Figure 7: Comparison of the different transient system responses to the step for the current feed-in by the PV inverter. The currents of both 3 phase systems are overlayed and synchronized. The occurrence of the step event is indicated separately for each setup.....	17
Figure 8: Comparison of the different transient systems response to the step of the voltage. The voltage of both 3 phase systems are overlayed and synchronized. The occurrence of every step event is indicated for each setup separately. Neither system shows a significant amount of disturbance	18
Figure 9: Comparison of the different system responses to the deviation voltage step. The reference curve is constructed by using the steady state results for given Q(U)-control. For system setup B varying time constants T_C for the Q(U) controller of PV inverter are presented. The depicted values are RMS-values calculated on a 1 period time frame. The dashed line represents the values for 1.05 p.u. as well as 1.08. p.u. which in turn are the setpoints for the break of the slope of the Q(U) controller.	19
Figure 10: Comparison of the different system responses to the deviation voltage ramp with the raise from 1.04 to 1.08 p.u. at the slack node over the course of 10 minutes. The thermal overload of the PI of system setup A is indicated.....	20
Figure 11: Comparison of the coordinated P(U) control governed by the EDCC and the Q(U) control of the inverter. Control characteristics are represented by the purple, respectively green lines	21
Figure 12: Transmitted Readings (EDCC) and independent measurements (IMD) for a time period with activated P(U) control algorithm.....	21
Figure 13: Illustration of the cycle time t_{PHIL} for system setup B for use in the evaluations of Phase 1 as well as for use in Phase 2. The white circle represents the median of the violin plot, the bold line represent the interquartile range and a density representation.....	22

8.2 List of Tables

Table 1: Requierments for the Setup.....	8
Table 2: Comparison of different domains using the X-in-the-loop concept for system testing with the focus on the energy sector.....	9

9 References

- [1] Smart Grids-Plattform Baden-Württemberg e.V., *C/Sells - Guiding principle*. [Online] Available: <https://www.csells.net/en/about-c-sells/guiding-principle.html>.
- [2] L. Martini *et al.*, "Grid of the future and the need for a decentralised control architecture: the web-of-cells concept," *CIGRED - Open Access Proceedings Journal*, vol. 2017, no. 1, pp. 1162–1166, 2017.
- [3] T. Strasser *et al.*, "Towards holistic power distribution system validation and testing--an overview and discussion of different possibilities," *e & i Elektrotechnik und Informationstechnik*, vol. 134, no. 1, pp. 71–77, 2017.
- [4] E. de Jong *et al.*, *European White Book on Real-Time Power Hardware-in-the-loop testing*. Kassel: DERlab e.V., 2012.
- [5] F. Lehfuss *et al.*, "Comparison of multiple power amplification types for power Hardware-in-the-Loop applications," in *2012 Complexity in Engineering (COMPENG). Proceedings*, Aachen, Germany, Jun. 2012 - Jun. 2012, pp. 1–6.
- [6] M. D. Omar Faruque *et al.*, "Real-Time Simulation Technologies for Power Systems Design, Testing, and Analysis," *IEEE Power Energy Technol. Syst. J.*, vol. 2, no. 2, pp. 63–73, 2015.
- [7] X. Guillaud *et al.*, "Applications of Real-Time Simulation Technologies in Power and Energy Systems," *IEEE Power Energy Technol. Syst. J.*, vol. 2, no. 3, pp. 103–115, 2015.
- [8] B. Lundstrom, S. Chakraborty, G. Lauss, R. Brundlinger, and R. Conklin, "Evaluation of system-integrated smart grid devices using software- and hardware-in-the-loop," in *2016 IEEE Power & Energy Society Innovative Smart Grid Technologies Conference (ISGT)*, Minneapolis, MN, USA, Sep. 2016 - Sep. 2016, pp. 1–5.
- [9] C. Holt, A. Kong, A. St. Leger, and D. Bennett, "Communications network emulation for smart grid test-bed," in *2016 IEEE Power and Energy Society General Meeting (PESGM)*, Boston, MA, USA, Jul. 2016 - Jul. 2016, pp. 1–5.
- [10] D. Babazadeh, M. Chenine, K. Zhu, L. Nordstrom, and A. Al-Hammouri, "A platform for wide area monitoring and control system ICT analysis and development," in *2013 IEEE Grenoble Conference*, Grenoble, France, Jun. 2013 - Jun. 2013, pp. 1–7.
- [11] Federal Office for Information Security (BSI), *Technical Guideline BSI TR-03109 SMART ENERGY*: Federal Office for Information Security (BSI), 2013.
- [12] International Electrotechnical Commission (IEC), *IEC 61850 Part 7-4: Basic communication structure - Compatible logical node classes and data object classes*, 2010.

10 References to Technical Data Sheets

- [13] Spitzenberger & Spies GmbH & Co. KG, Data Sheet: PAS series of 4-Quadrant Amplifiers, online: <https://www.spitzenberger.de/web/1002>, accessed on 2018-08-24
- [14] OPAL-RT TECHNOLOGIES Inc., Product Sheet: Real-Time Simulation Solutions for Power Grids and Power Electronics, https://www.opal-rt.com/wp-content/themes/enfold-opal/pdf/L00161_0260.pdf
- [15] Fronius International GmbH, Data Sheet: FRONIUS Symo Series, online: http://www.fronius.com/~/downloads/Solar%20Energy/Datasheets/SE_DS_Fronius_Symo_DE.pdf, accessed on 2018-08-28
- [16] Dewetron GmbH, Data Sheet: DEWE -800, online: https://www.dewetron.com/wp-content/uploads/2016/05/dewetron_dewe-800_e-1.pdf, accessed on 2018-08-28
- [17] DIgSILENT GmbH, Data Sheet: PowerFactory 2018, online: <https://www.digsilent.de/en/downloads.html>, accessed on 2018-08-28
- [18] Regatron AG, Data Sheet: TC.ACS PROGRAMMABLE AC SOURCE-SINK SERIES, online: <https://www.regatron.com/service/download/brochures/tc.acs-series-brochure.pdf>, accessed on 2018-08-28
- [19] Janitza electronics GmbH, Data Sheet: Universal Measuring Device UMG 96 - Operating instructions, online: <https://www.janitza.de/betriebsanleitungen.html?file=files/download/manuals/current/UMG96/Janitza-Manual-UMG96-all-versions-en.pdf>, accessed on 2018-08-28
- [20] KNIME Analytics Platform, online: <https://www.knime.com/knime-software/knime-analytics-platform>, accessed on 2018-10-28